RESEARCH ARTICLE

Normative Values of Neuromelanin-Sensitive MRI Signal in Older Adults Obtained Using a Turbo Spin Echo Sequence

Rami Al Haddad, MS,[1] Mira Chamoun, PhD,[2] Christine L. Tardif, PhD,[3] Synthia Guimond, PhD,[1] Guillermo Horga, MD, PhD,[4] Pedro Rosa-Neto, MD, PhD,[2,3] and Clifford M. Cassidy, PhD[1,2*]

Background: The integrity and function of catecholamine neurotransmitter systems can be assessed using neuromelanin-sensitive MRI (NM-MRI). The relevance of this method to neurodegenerative and psychiatric disorders is becoming increasingly evident, and it has potential as a clinical biomarker.
Purpose: To support future application of NM-MRI as a clinical biomarker by defining the normative range of NM-MRI signal and volume metrics in cognitively normal older adults.
Study Type: Prospective.
Population: A total of 152 cognitively normal older adults aged 53–86 years old, including 41 participants who had follow-up NM-MRI data collected 9–16 months later.
Field Strength/Sequence: A 3.0 T; NM-MRI turbo spin echo and T1-weighted magnetization-prepared rapid acquisition with gradient echo sequences.
Assessment: NM-MRI images were processed to yield summary measures of volume and signal (contrast-to-noise ratio, CNR) for the substantia nigra (SN) and locus coeruleus (LC) using a recently developed software employing a fully automated algorithm. Change in these metrics over time was also assessed.
Statistical Tests: Mean and standard deviation of NM-MRI metrics were calculated; change over time was tested for significance using 1-sample t-tests. P values < 0.05 were considered statistically significant.
Results: At baseline SN signal (CNR) was 10.02% (left) and 10.28% (right) and LC signal was 24.71% (left) and 20.42% (right). Baseline SN volume was 576 mm^3 (left) and 540 mm^3 (right) and LC volume was 6.31 mm^3 (left) and 6.30 mm^3 (right). The only NM-MRI metric showing significant change was a decrease in left SN volume ($t_{40} = -2.57$, $P = 0.014$).
Data Conclusion: We report normative values for NM-MRI signal and volume in the SN and LC of cognitively normal older adults and explore their change over time. These values may help future efforts to use NM-MRI as a clinical biomarker by facilitating identification of patients with extreme NM-MRI values.
Level of Evidence: 2.
Technical Efficacy Stage: 1.

J. MAGN. RESON. IMAGING 2022.

Neuromelanin-sensitive MRI (NM-MRI) is an increasingly popular method to interrogate the integrity and function of the brain's major catecholamine nuclei, the dopaminergic substantia nigra (SN), and the noradrenergic locus coeruleus (LC).[1–5] The method has been most broadly applied in research studies of neurodegenerative illnesses such

View this article online at wileyonlinelibrary.com. DOI: 10.1002/jmri.28530

Received Jun 28, 2022, Accepted for publication Nov 2, 2022.

*Address reprint requests to: C.M.C., The Royal Institute of Mental Health Research, 1145 Carling Avenue, room 5414, Ottawa, Ontario, Canada. E-mail: clifford.cassidy@theroyal.ca

From the [1]The Institute of Mental Health Research, University of Ottawa, Ottawa, Ontario, Canada; [2]McGill University Research Centre for Studies in Aging, Montreal, Quebec, Canada; [3]Montreal Neurological Institute, McGill University, Montreal, Quebec, Canada; and [4]Department of Psychiatry, Columbia University, New York City, New York, USA

Additional supporting information may be found in the online version of this article

as Parkinson's disease and Alzheimer's disease as a marker of degeneration of these nuclei.[2,3,6,7] More recently, it has been applied in psychiatric conditions, where the NM-MRI signal has been shown to correlate with important aspects of psychopathology, consistent with evidence that the signal may assay aspects of the function of these neurotransmitter systems, even in the absence of neurodegeneration.[1,8,9] While the extent of neuromelanin's contribution to the NM-MRI signal is debated, a correlation has been observed between the signal and NM concentration in post-mortem midbrain.[1,8,10,11]

Many research studies support the potential of NM-MRI as a neuroimaging biomarker that could prove useful in clinical applications such as diagnosis or treatment of neurodegenerative and psychiatric disorders.[2,7,8,12] Supporting such applications, NM-MRI has excellent test–retest reliability with intraclass correlation coefficient (ICC) values of 0.95 or higher, suggesting that quantitative measures of NM-MRI signal can be consistently obtained with minimal error.[1,13,14] Nevertheless, there are also challenges that must be overcome to support its use as a biomarker.[8,11,15] First of all, to be used universally, it is necessary for NM-MRI metrics from different scanners and different sites to be comparable.[8,10,14,16] This is challenging because, in many applications, it is the signal contrast of the nuclei that would be the principal metric of interest.[10,13,17] Compared to, for instance, volumetric measures, signal contrast is more sensitive to factors such as scanner model, pulse sequence, acquisition parameters, and head coil.[8,14] Thus, these sources of variability should be minimized and also data harmonization methods such as ComBat, a batch effect correction tool commonly used in genomics, should be applied as part of data processing in the context of multisite studies or when comparing NM-MRI measurements to an external standard.[1,18,19] The second challenge is the observation that the NM-MRI signal increases with age, sharply during childhood, reaching a plateau in middle age, and then declining in later life.[20–22] These findings may be due to NM's tendency to gradually accumulate in the cell bodies of catecholamine neurons, only being cleared from the tissue after cell death.[3,20,23,24] Indeed, post-mortem observations have found a similar pattern of age-related change in the accumulation of NM in these nuclei.[25–27] As a result, a signal contrast that is relatively high for the SN of a teenager would be relatively low for a middle-aged adult.[20–22,28] Therefore, age is a critical factor that should be adjusted for when using NM-MRI.[20,29] With these challenges in mind, future NM-MRI work using standard methods of acquisition and analysis and stratifying a large sample of participants by age would be well positioned to determine the normative range of SN and LC contrast ratios and volumes in healthy people of all ages. In the context of its potential use as a biomarker, access to a standardized, age-adjusted normative range of NM-MRI metrics is essential to identify patients at the extreme ends of the range, presumably those who may require clinical intervention. While a large sample spanning the entire lifespan will be ultimately necessary to provide granular age adjustment, in the current study, we propose that a smaller sample of older subjects will be adequate to approximate the normative range of NM-MRI metrics in cognitively normal adults over 53 years old, this being a clinically relevant age given the emergence of common neurodegenerative conditions in older adults.[30–32]

Thus, the aim of this study was to advance NM-MRI toward its potential use as a biomarker by conducting a NM-MRI study in a sample of cognitively normal older adults using standard methods for acquisition and analysis via a fully automated software for processing NM-MRI images that was recently developed following methods used by our group previously.[1,7,33] The aim was to report measures of NM-MRI signal and volume for the SN and LC, as well as to provide preliminary evidence of their change over time in this population.

Methods

Participants

After obtaining the Research Ethics Board approval, participants from the community were enrolled in the study. After obtaining written informed consent, participants had a detailed clinical assessment, including the Clinical Dementia Rating Scale (CDR) and Mini-Mental State Examination (MMSE), administered at baseline and follow-up assessments.[34,35] All participants in the study were deemed to be cognitively unimpaired, with no objective cognitive impairment and a CDR score of 0. Participants were excluded if they had other inadequately treated conditions, active substance abuse, recent head trauma, or major surgery, or if they had MRI safety contraindication. A sample of 152 from participants (53–86 years old) were enrolled for baseline scanning and 41 returned for their follow-up scan around 9–16 months after the first scan.

MRI Acquisition

All neuroimaging data were acquired on a 3 T Prisma-Fit scanner (Siemens, Erlangen, Germany). NM-MRI images were collected via a turbo spin echo (TSE) sequence with the following parameters: repetition time (TR) = 600 msec; echo time (TE) = 10 msec; flip angle = 120°; turbo factor = 4; in-plane resolution = 0.6875×0.6875 mm^2; partial brain coverage overlaying the pons and midbrain with field of view (FoV) = 165×220 mm^2; number of slices = 20; slice thickness = 1.8 mm; number of averages = 7; acquisition time = 8.45 minutes. The image stack was aligned perpendicular to the axis of the pontine brainstem, providing coverage of the brainstem from the posterior recess of the fourth ventricle at the caudal extent to a point slightly above the

floor of the third ventricle at the rostral extent. Whole-brain, T1-weighted MR images (resolution = 1 mm, isotropic) were acquired using an MPRAGE sequence for preprocessing of the NM-MRI. Quality of MRI images was visually inspected for artifacts immediately upon acquisition by the MR technologists (with over 15 years of experience). In case of suboptimal image quality, scans were repeated, time permitting.

Preprocessing of NM-MRI Images

Preprocessing of NM-MRI images was performed using a fully automated, cloud-based software package, NM-101, version 1.0.3 (Terran Biosciences. New York, NY, USA). The initial algorithm steps were necessary for processing of both LC and SN metrics. These included brain extraction of T1-weighted images, spatial normalization of T1-weighted images into standardized MNI space, rigid coregistration of NM-MRI images to T1-weighted images, and spatial normalization of NM-MRI images into MNI space (resampled at 1 mm, isotropic). All steps to calculate all LC and SN metrics were fully automatic.

To calculate SN metrics from the spatially normalized images, we used an approach adopted by Wengler et al.[1,13,14,33] Note that here we refer to the SN, but our SN mask also contains the dopaminergic ventral tegmental area (VTA), and thus the structure assayed here could also be referred to as the SN-VTA complex. Intensity normalization determined contrast-to-noise ratio (CNR) for each subject and voxel as the relative change in NM-MRI signal intensity from a reference region of white matter tracts known to have minimal NM content, the crus cerebri. Images were then spatially smoothed with a 1-mm full-width-at-half-maximum Gaussian kernel. Finally, an overinclusive mask of the SN in MNI space was applied that ensured inclusion of the SN and VTA for all individuals. SN signal was calculated by averaging CNR values for all SN voxels on the left and right sides of this mask. SN volume on the left and right sides was calculated by an automated threshold-based segmentation identifying SN voxels in MNI space above a fixed intensity threshold and multiplying by the volume of one voxel (1 mm^3). The intensity threshold was equal to two times the standard deviation calculated from all reference region voxels of all subjects after trimming reference region voxels with extreme intensity values.[14]

To calculate LC metrics from the raw NM-MRI images, we used an approach similar to a published method[7]; An LC search space (referred to as the LC search mask, spanning 5 mm in the rostrocaudal axis from MNI space) was created to cover the middle LC (where signal intensity is highest and automated segmentation accuracy is very high, ~99% accuracy) and exclude the rostral and caudal portions of the structure.[7] This LC search mask was then warped to NM-MRI space using the inverse transformations generated in the spatial normalization and rigid coregistration steps. This warped LC search mask defined a search space wherein to find the LC for each participant. A cluster-forming algorithm was used to segment the LC within this space. This was repeated on each side (left and right) and axial slice. To minimize partial volume effects, only the brightest of these voxels (peak intensity voxel) was retained for calculation of LC signal on each side and slice (on the assumption that the peak intensity voxel had the highest fraction of LC tissue). CNR for each voxel in a given axial slice was then calculated as the relative difference in NM-MRI signal intensity from the portion of a reference region in the same axial slice. We used a reference region with low NM concentration, the central pons.[36] The central pons mask was transformed from MNI space to NM-MRI space for each participant. LC signal was calculated by averaging CNR values from the all peak intensity LC voxels on the left and right sides.

LC volume was calculated using an automated threshold-based segmentation in native space. The LC voxels above a fixed intensity threshold were retained on each side for every axial slice, then divided by the number of axial slices to estimate average LC voxels per slice, and then multiplied by the area per voxel. The resulting area measure was multiplied by a fixed LC length (equal to the length of the LC search mask in MNI space, 5 mm). Therefore, all variability in our measure of LC volume was due to variability in LC area, with rostrocaudal length fixed due to the inability of our method to precisely measure this dimension. This was repeated on both the left and right sides. This method for LC volume calculation was designed to capture volume loss in neurodegenerative illness, consistent with the intent of the NM-101 software. The intensity threshold was set as the maximum value where no cognitively normal participants had floor values (0 voxels) for LC volume. Many participants had ceiling values for LC volume using these thresholds. Due to left–right asymmetry in the NM-MRI images, different thresholds were applied on the left and right sides.

Statistical Analysis

All NM-MRI metrics generated by NM-101 software were analyzed using Matlab software. Normality was assessed using Lilliefors test (alpha = 0.05). Linear regression was used to relate baseline and change NM-MRI metrics to age. Change metrics for all NM-MRI metrics were calculated by subtracting NM-MRI metrics at baseline from the same metrics at follow-up, 9–16 months later. To determine if these change metrics significantly differed from 0, 1-sample t-tests were conducted.

Results

Section 1: Normative Metrics: Baseline

The sample included 152 adults aged between 53 and 86 years at baseline (see Fig. S1 for age distribution). Mean

TABLE 1. Summary NM-MRI Metrics at Baseline and Change Over 1 year

		SN			LC		
		Baseline	Change Over Time	Tstat (Change Over Time)	Baseline	Change Over Time	Tstat (Change Over Time)
Signal (CNR)	Left	10.02 ± 1.48	−0.39 ± 1.32	−1.89	24.71 ± 4.88	0.67 ± 3.29	1.28
	Right	10.28 ± 1.51	−0.30 ± 1.18	−1.61	20.42 ± 4.95	−0.62 ± 2.92	−1.35
Volume (mm^3)	Left	576.4 ± 83.0	−30.44 ± 75.9	−2.57*	6.31 ± 1.22	0.27 ± 0.92	1.83
	Right	540 ± 74.9	−17.21 ± 64.2	−1.72	6.30 ± 1.20	0.30 ± 1.37	1.41

Baseline $n = 152$, Follow-up $n = 41$. CNR = contrast-to-noise ratio; SN = substantia nigra; LC = locus coeruleus.
*$P = 0.014$.

age was 71.2 ± 5.9 years, mean years of education was 15.3 ± 35, mean score on the mini-mental exam was 29.2 ± 1.4, 50 participants were male (32.9%), and 110 participants were Caucasian (86.6%; see Table S1 for demographic characteristics of the full sample and comparison with the subsample having follow-up data). Baseline SN signal had CNR values of 10.02% (left SN) and 10.28% (right SN) and baseline LC signal was 24.71% (left) and 20.42% (right; see Table 1 for all signal and volume measures). All signal measures were normally distributed at baseline. This was not the case for all volume measures (consistent with our decision to set volume thresholds where many healthy individuals would be at or near the ceiling, this was particularly true of LC volume metrics). Refer to Table S2 for values of all baseline summary metrics for all participants and Table S3 for voxel-level values within the SN for all participants. Figure 1 shows an SN map illustrating voxelwise values for baseline SN signal and Fig. 2 shows the LC NM-MRI signal and mask placement.

Linear regression analyses showed that there were no significant relationships between NM-MRI signal or volume in the SN or LC with age (left SN signal, $P = 0.80$; right SN signal, $P = 0.17$; left SN volume, $P = 0.32$; right SN volume, $P = 0.14$; left LC signal, $P = 0.98$; right LC signal, $P = 0.71$; left LC volume, $P = 0.99$; right LC volume, $P = 0.91$; see Fig. S2 for scatterplots of these relationships).

Section 2: Change over Time

Follow-up images after approximately 1 year (9–16 months) were available for $n = 41$ participants ($n = 40$ for LC). Mean change in NM-MRI metrics over the year were negative (decreases over time) for SN and tended to be positive (increases) for LC (Table 1). There was a large amount of variability across subjects in all metrics with some subjects showing increases and some decreases over time. Similar to observations at baseline, change in signal metrics over time was normally distributed but change in volume measures was not. Only SN volume on the left side showed significant change over time across subjects (Table 1, 1-sample t-tests).

Linear regression analyses showed that there were no significant relationships between age and change metrics (left SN signal, $P = 0.96$; right SN signal, $P = 0.42$; left SN volume, $P = 0.57$; right SN volume, $P = 0.73$; left LC signal, $P = 0.16$; right LC signal, $P = 0.39$; left LC volume, $P = 0.73$; right LC volume, $P = 0.30$; see Fig. S2 for scatterplots of these relationships).

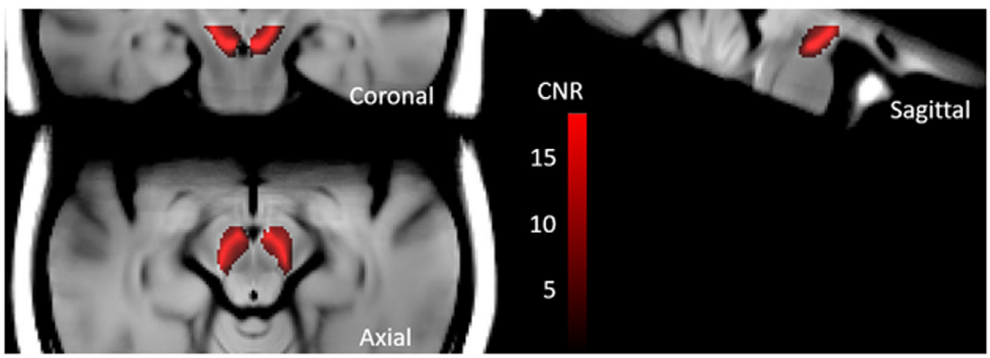

FIGURE 1: Mean NM-MRI signal from SN voxels at baseline in older adults overlaid on visualization template in MNI space. Signal is highest in the central SN (SN = substantia nigra).

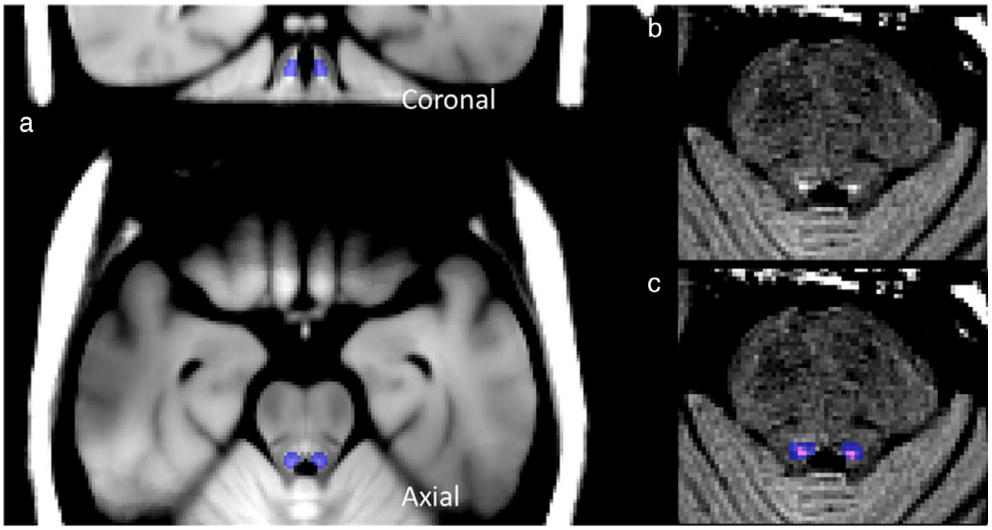

FIGURE 2: LC NM-MRI signal and mask placement. (a) Coronal and axial images showing the overinclusive LC mask (blue) overlaid on the visualization template. (b) Pons of a representative subject in native space. (c) Overlay of the overinclusive LC mask (blue) after transformation to native space. This larger mask is used as a search space to identify hyperintense LC voxels (pink; three adjacent voxels per side) (LC = locus coeruleus).

Discussion

Here, we use a fully automated algorithm to determine normative values for baseline NM-MRI signal and volume in the LC and SN and explore their change over time. Change metrics for NM-MRI summary metrics were largely nonsignificant but tended to decrease for SN metrics and increase for LC metrics.

We confirmed that there was no significant relation between our NM-MRI metrics and age. While we did see a decreasing trend in some of these metrics, consistent with evidence that NM-MRI metrics begin decreasing at some point in later life,[20] these effects were relatively weak, supporting the acceptability of collapsing across this age range. We also checked whether age significantly affected change metrics and found this was not the case suggesting that, similar to baseline metrics, collapsing across this age range may be acceptable when considering change metrics.

These normative values from cognitively normal older individuals could be useful if NM-MRI achieves its potential as a biomarker to support clinical decision-making. For instance, NM-MRI has been widely used in research studies in Parkinson's disease but could potentially be introduced to the clinic to assist with diagnosis or treatment monitoring by flagging individuals with low NM-MRI signal or with marked signal loss over time relative to the normal values from healthy individuals.[1,6,7,37] When possible, these normative values would be adjusted in a scanner-specific manner (eg using ComBat) to account for differences across scanners that could shift the range of the NM-MRI signal, even when parameters and equipment are closely matched between scanners.[18,19] The subject-level data provided in Supplementary Materials S1 could assist with this harmonization process.

Limitations

The small sample size prevented us from subdividing it into smaller age subgroups or dividing it by sex or other demographic factors. This was particularly true for the sample with follow-up data ($n = 41$). Due to this and the fact that there was a relatively large range in the duration of the follow-up interval, we do not consider this sample adequate to provide normative values for change over time but merely to give a very preliminary estimate of the magnitude of change over time of these metrics. Hence, we advise the longitudinal data to be interpreted with caution. Ideally, a future study should collect a substantially larger sample of people across the entire lifespan and carefully sample to get equal age and sex distribution to allow division of the sample into age subgroups (perhaps 10 years or smaller) with equal representation. This would allow for more fine-grained norms, potentially narrowing their range and facilitating identification of patients at risk of neurodegenerative or perhaps psychiatric illness. Nevertheless, it is reassuring that we did not observe significant age-related change in any of our summary NM-MRI metrics over the age range employed here, supporting the utility of these norms for adults aged between 53 and 86 years old.

In addition, the normative values presented in this study are not only limited to a specific population (older adults) but also by the NM-MRI acquisition protocol. While they should be robust to small changes in sequence parameters, assuming the values are harmonized using ComBat or a similar approach, they cannot be applied universally to any NM-MRI acquisition. We have reported values using a TSE sequence and these cannot be compared to values obtained using the other commonly used sequence for NM-MRI,

a 2D gradient recalled echo sequence with magnetization transfer pulse (2D-GRE with MT).[1,4] We selected the TSE sequence here given our objective of providing norms that could be clinically useful and the fact that on some scanner brands a developer-made 2D-GRE sequence is needed, making the latter sequence a step further removed from clinical implementation. While the 2D-GRE with MT has shown superior contrast and reproducibility compared to a TSE sequence, the TSE sequence nonetheless generally showed good contrast and reproducibility.[14] The extent to which these different sequences are sensitive to NM as opposed to other properties of catecholamine neurons (eg the increased free water fraction in their large cell bodies) has not been adequately tested and such information about NM specificity could help settle the debate about which NM-MRI sequence is best.[1,10] When used as a marker of neurodegeneration this point may be less critical since not only neuromelanin but any other contrast-promoting factor within the cells is likely to be lost when they die.

Furthermore, some of the volume metrics were not normally distributed. In the case of the LC, this was due to our decision to select an intensity threshold where none of our cognitively normal individuals would have an LC volume equal to zero. We felt that this would better support the objective of our software to detect neurodegeneration; however, consequently, it has restricted the ability to observe variability in LC volume in healthy individuals.

Finally, while it is not surprising that our longitudinal data did not reveal a significant change over time for most metrics (given little change within this time interval in studies of late-life age effects), it is somewhat surprising that the some LC metrics tended to weakly increase rather than decrease.[19,25,26] Prior studies have shown LC signal increases with age in early life and decreases in late life.[25,26] Differences between our study and prior work that could explain this difference include our rigorous screening to exclude individuals at risk of dementia (more likely to have early LC degeneration[30]), and our focus on only the middle portion of the LC, excluding the rostral and caudal ends of the structure.

Conclusion

Our results might provide normative values of NM-MRI signal and volume for the SN and LC in cognitively normal older adults. Such norms represent one of the necessary components in the effort to introduce this promising neuroimaging method into the clinic as a biomarker for neurodegenerative and psychiatric disorders.

References

1. Cassidy CM, Zucca FA, Girgis RR, et al. Neuromelanin-sensitive MRI as a noninvasive proxy measure of dopamine function in the human brain. Proc Natl Acad Sci 2019;116(11):5108-5117.
2. Wang J, Li Y, Huang Z, et al. Neuromelanin-sensitive magnetic resonance imaging features of the substantia nigra and locus coeruleus in de novo Parkinson's disease and its phenotypes. Eur J Neurol 2018; 25(7):949-e73.
3. Fedorow H, Tribl F, Halliday G, Gerlach M, Riederer P, Double KL. Neuromelanin in human dopamine neurons: Comparison with peripheral melanins and relevance to Parkinson's disease. Prog Neurobiol 2005;75(2):109-124.
4. Chen X, Huddleston DE, Langley J, et al. Simultaneous imaging of locus coeruleus and substantia nigra with a quantitative neuromelanin MRI approach. Magn Reson Imaging 2014;32(10):1301-1306.
5. Simões RM, Castro Caldas A, Grilo J, et al. A distinct neuromelanin magnetic resonance imaging pattern in parkinsonian multiple system atrophy. BMC Neurol 2020;20(1):432.
6. Bae YJ, Kim JM, Sohn CH, et al. Imaging the substantia Nigra in Parkinson disease and other parkinsonian syndromes. Radiology 2021; 300(2):260-278.
7. Cassidy CM, Therriault J, Pascoal TA, et al. Association of locus coeruleus integrity with Braak stage and neuropsychiatric symptom severity in Alzheimer's disease. Neuropsychopharmacology 2022;47(5): 1128-1136.
8. Sulzer D, Cassidy C, Horga G, et al. Neuromelanin detection by magnetic resonance imaging (MRI) and its promise as a biomarker for Parkinson's disease. NPJ Park Dis 2018;4:11.
9. Paloyelis Y, Mehta MA, Kuntsi J, Asherson P. Functional magnetic resonance imaging in attention deficit hyperactivity disorder (ADHD): A systematic literature review. Expert Rev Neurother 2007;7(10):1337-1356.
10. Priovoulos N, van Boxel SCJ, Jacobs HIL, et al. Unraveling the contributions to the neuromelanin-MRI contrast. Brain Struct Funct 2020;225(9): 2757-2774.
11. Trujillo P, Summers PE, Ferrari E, et al. Contrast mechanisms associated with neuromelanin-MRI. Magn Reson Med 2017;78(5):1790-1800.
12. Wang L, Yan Y, Zhang L, Liu Y, Luo R, Chang Y. Substantia nigra neuromelanin magnetic resonance imaging in patients with different subtypes of Parkinson disease. J Neural Transm (Vienna) 1996;128(2): 171-179.
13. Wengler K, He X, Abi-Dargham A, Horga G. Reproducibility assessment of neuromelanin-sensitive magnetic resonance imaging protocols for region-of-interest and voxelwise analyses. Neuroimage 2020;1(208): 116457.
14. van der Pluijm M, Cassidy C, Zandstra M, et al. Reliability and reproducibility of neuromelanin-sensitive imaging of the substantia Nigra: A comparison of three different sequences. J Magn Reson Imaging 2021; 53(3):712-721.
15. Liu Y, Li J, He N, et al. Optimizing neuromelanin contrast in the substantia nigra and locus coeruleus using a magnetization transfer contrast prepared 3D gradient recalled echo sequence. Neuroimage 2020; 1(218):116935.
16. Turesky TK, Vanderauwera J, Gaab N. Imaging the rapidly developing brain: Current challenges for MRI studies in the first five years of life. Dev Cogn Neurosci 2021;1(47):100893.
17. Horga G, Wengler K, Cassidy CM. Neuromelanin-sensitive magnetic resonance imaging as a proxy marker for catecholamine function in psychiatry. JAMA Psychiat 2021;78(7):788-789.
18. Wengler K, Cassidy C, van der Pluijm M, et al. Cross-scanner harmonization of neuromelanin-sensitive MRI for multisite studies. J Magn Reson Imaging 2021;54(4):1189-1199.
19. Johnson M, Purdom E. Clustering of mRNA-Seq data based on alternative splicing patterns. Biostatistics 2017;18(2):295-307.
20. Xing Y, Sapuan A, Dineen RA, Auer DP. Life span pigmentation changes of the substantia nigra detected by neuromelanin-sensitive MRI. Mov Disord off J Mov Disord Soc 2018;33(11):1792-1799.
21. Vila M. Neuromelanin, aging, and neuronal vulnerability in Parkinson's disease. Mov Disord 2019;34(10):1440-1451.

22. Zucca FA, Vanna R, Cupaioli FA, et al. Neuromelanin organelles are specialized autolysosomes that accumulate undegraded proteins and lipids in aging human brain and are likely involved in Parkinson's disease. Npj Park Dis 2018;4(1):1-23.

23. Mahul-Mellier AL, Burtscher J, Maharjan N, et al. The process of Lewy body formation, rather than simply α-synuclein fibrillization, is one of the major drivers of neurodegeneration. Proc Natl Acad Sci 2020; 117(9):4971-4982.

24. Carballo-Carbajal I, Laguna A, Romero-Giménez J, et al. Brain tyrosinase overexpression implicates age-dependent neuromelanin production in Parkinson's disease pathogenesis. Nat Commun 2019;10(1):973.

25. Sasaki M, Shibata E, Tohyama K, et al. Neuromelanin magnetic resonance imaging of locus ceruleus and substantia nigra in Parkinson's disease. Neuroreport 2006;17(11):1215-1218.

26. Shibata E, Sasaki M, Tohyama K, et al. Age-related changes in locus ceruleus on neuromelanin magnetic resonance imaging at 3 tesla. Magn Reson Med Sci 2006;5(4):197-200.

27. Liu KY, Acosta-Cabronero J, Cardenas-Blanco A, et al. In vivo visualization of age-related differences in the locus coeruleus. Neurobiol Aging 2019;74:101-111.

28. Zucca FA, Basso E, Cupaioli FA, et al. Neuromelanin of the human substantia nigra: An update. Neurotox Res 2014;25(1):13-23.

29. Wieland L, Fromm S, Hetzer S, Schlagenhauf F, Kaminski J. Neuromelanin-sensitive magnetic resonance imaging in schizophrenia: A meta-analysis of case-control studies. Front Psychiatry 2021;12.

30. Mendez MF. Early-onset Alzheimer disease and its variants. Contin Minneap Minn 2019;25(1):34-51.

31. Zafar S, Yaddanapudi SS. Parkinson disease. *StatPearls [Internet]*. Treasure Island, FL: StatPearls Publishing; 2022.

32. Hou Y, Dan X, Babbar M, et al. Ageing as a risk factor for neurodegenerative disease. Nat Rev Neurol 2019;15(10):565-581.

33. Wengler K, Ashinoff BK, Pueraro E, Cassidy CM, Horga G, Rutherford BR. Association between neuromelanin-sensitive MRI signal and psychomotor slowing in late-life depression. Neuropsychopharmacol 2021;46(7):1233-1239.

34. Nyunt MSZ, Chong MS, Lim WS, Lee TS, Yap P, Ng TP. Reliability and validity of the clinical dementia rating for community-living elderly subjects without an informant. Dement Geriatr Cogn Disord Extra 2013; 3(1):407-416.

35. Arevalo-Rodriguez I, Smailagic N, Roqué i Figuls M, et al. Mini-Mental State Examination (MMSE) for the detection of Alzheimer's disease and other dementias in people with mild cognitive impairment (MCI). Cochrane Database Syst Rev 2015;2015(3):CD010783.

36. Dordevic M, Müller-Fotti A, Müller P, Schmicker M, Kaufmann J, Müller NG. Optimal cut-off value for locus coeruleus-to-pons intensity ratio as clinical biomarker for Alzheimer's disease: A pilot study. J Alzheimers Dis Rep 2017;1(1):159-167.

37. Cassidy C, Celebi S, Savard M, Chamoun M, Tardif CL, Rosa-Neto P. Neuromelanin-sensitive MRI as an index of norepinephrine system integrity in healthy aging, mild cognitive impairment, and Alzheimer's disease. Biol Psychiatry 2020;87(9):S424-S425.